Journal of Saudi Chemical Society (2019) **23**, 1060–1069

King Saud University

Journal of Saudi Chemical Society

www.ksu.edu.sa
www.sciencedirect.com

ORIGINAL ARTICLE

Synthesis of environmentally friendly, magnetic acid-type calix[4]arene catalyst for obtaining Biginelli adducts

Carlos Henrique Callegario Zacchi [a], Sara Silveira Vieira [a], José Domingos Ardisson [b], Maria Helena Araujo [a,*], Ângelo de Fátima [a,*]

[a] *Universidade Federal de Minas Gerais, Instituto de Ciências Exatas, Departamento de Química, Belo Horizonte, MG 31270-901, Brazil*
[b] *Laboratório de Física Aplicada, Centro de Desenvolvimento da Tecnologia Nuclear, Belo Horizonte, MG 30123-970, Brazil*

Received 6 April 2019; revised 15 May 2019; accepted 16 May 2019
Available online 8 June 2019

KEYWORDS

Fe_3O_4 nanoparticles;
p-sulfonic acid calix[4]arene;
Magnetic acid catalyst;
Biginelli adducts

Abstract An immobilized *p*-sulfonic acid calix[4]arene was synthesized on the surface of silica-coated Fe_3O_4 nanoparticles. Due to the combination of the magnetic recovery and the acid properties, it acted as a robust, safe and environmentally friendly catalyst for the one-pot synthesis of Biginelli adducts under microwave irradiation and solvent-free conditions. A series of Biginelli adducts were obtained in moderate to excellent yields, and most importantly, the catalyst could be easily recovered by an external magnet and reused five times without significant loss of catalytic activity (*ca.* 80% yield for all reuses using 0.64 mol% of the catalyst).

1. Introduction

Catalysis is a crucial component of green chemistry in which some of the challenges are the design and use of environmentally friendly catalysts in organic reactions [1,2]. A maintainable and environmentally friendly catalyst must have specific features, such as selectivity, high stability, efficient recovery, and good recyclability [3–7].

Catalysts are conventionally categorized into homogeneous and heterogeneous types in which the former has advantages over the latter by possessing good activity, selectivity and accessible mechanistic studies leading to catalyst optimization. However, the separation of homogeneous catalysts from reaction media may be difficult, time-consuming and a problem for application in industry, particularly the pharmaceutical industry, where metal contamination from a metallic catalyst in the final product is not acceptable [8,9].

Heterogenization of homogeneous catalysts with a solid support to produce heterogeneous catalytic systems is an effective approach to accomplish the separation of catalysts. Indeed, solid catalysts have a number of advantages over

* Corresponding authors.
E-mail addresses: mharaujo@ufmg.br (M.H. Araujo), adefatima@qui.ufmg.br (Â. de Fátima).
Peer review under responsibility of King Saud University.

ELSEVIER Production and hosting by Elsevier

https://doi.org/10.1016/j.jscs.2019.05.005
1319-6103

homogeneous catalysts since they can be easily removed from the reaction, allowing their regeneration and reuse, minimizing metal traces in the product, and improving handling and process control [2–5].

Beyond the heterogeneous property of the catalyst, magnetic separable catalyst particles are of great interest for researchers due to easy magnetic separation from reaction mixtures, facilitating repeated catalyst use and allowing savings of energy and materials, thus decreasing the target product costs [7,10,11].

Magnetite (Fe_3O_4) is an important magnetic material derived from iron. This oxide is notable in relation to other magnetic oxides because it is easily obtained by means of several techniques well described in the literature, such as coprecipitation [12], hydrothermal [13], solvothermal, thermal decomposition [14], sol-gel [15,16], mechanochemical [17] and precipitation [18].

Indeed, the use of magnetite as a support for catalysts is a growing field in heterogeneous catalysis due to its easy preparation and very active surface for adsorption or immobilization of metals and/or ligands. Magnetite-supported organocatalysts may be easily separated from the reaction mixture by magnetic means, thereby generating a more sustainable catalyst [11,19,20].

Calix[*n*]arenes are macrocyclic compounds of phenolic units linked by methylene groups at the 2,6-positions and are recognized host-guest catalysts that showed promising results as homogenous and heterogeneous catalysts [21–26]. In previous works, our research group used *p*-sulfonic acid calix[4]arene (**CX4**; Fig. 1A) as a homogeneous catalyst to obtain julolidine [27,28], quinolones [29,30], xanthenones [31] and 3,4-dihydropyrimidin-2(1*H*)-ones/-thiones (also named Biginelli adducts) [32–35].

In addition to the excellent performance of calixarenes as homogeneous catalysts [22,36], they have also been used in their heterogeneous form in different materials [37]. For instance, gold-polypyrrole doped with 4-sulfocalix[4]arene nanocomposites were employed as electrochemical sensors [38], *para*-sulfonatocalix[4]arene-modified silver nanoparticles were shown to be selective colorimetric histidine probes [39], composites made of nanoparticles of mesoporous silica allylcalix[4]arene hybrids were used for the sustained release of doxorubicin into cancer cells [40], calix[4]arene magnetic nanoparticles were used for encapsulation of *Candida rugosa* lipase, improving the enzyme catalytic properties [41], and calixarene immobilized onto magnetic nanoparticle surfaces was used as an excellent extractant for metals [42].

Heterogeneous calixarene-based catalysts have, potentially, a series of advantages over the homogenous ones; however, the use of the former is still to be explored. To the best of our knowledge, only two examples of heterogeneous calixarene-based magnetic catalyst systems are described in the literature

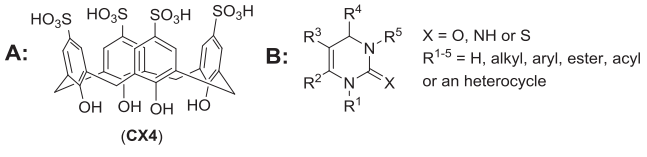

Fig. 1 (A) Chemical structure of *p*-sulfonic acid calix[4]arene (**CX4**) and (B) general chemical structure of Biginelli adducts.

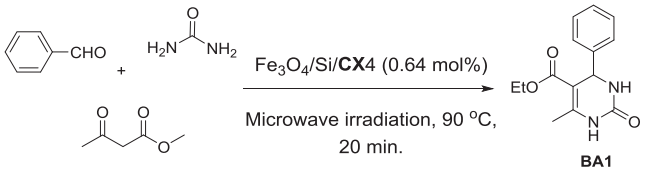

Scheme 1 The Biginelli model used to optimizing the reaction conditions using the catalyst Fe_3O_4/Si/**CX4**.

[26]: calixarene-proline functionalized iron oxide magnetite nanoparticles were described as organocatalysts in an aldol reaction [43], and immobilizing calix[*n*]arene sulfonic acids onto silica-coated magnetic nanoparticles catalyzed the coupling of electron-rich arenes with some alcohols in water [44].

Our main interest in Biginelli adducts (Fig. 1B) is due to their promising pharmacological properties, which include antiviral, antitumor, anti-inflammatory, antibacterial, antifungal, anti-epileptic, antimalarial, and antileishmanial properties, among others [34,45].

Herein, we report a novel application of an immobilized *p*-sulfonic acid calix[4]arene (**CX4**) onto silica-based magnetite particle (Fe_3O_4/Si) surfaces for the Biginelli reaction, a multicomponent reaction (MCR). Our results showed that Fe_3O_4/Si/**CX4** is a reusable environmentally friendly catalyst to obtain Biginelli adducts under solvent-free conditions and microwave irradiation (IMO) (Scheme 1).

2. Experimental

2.1. Materials

The reagents used in the synthesis of the heterogeneous catalyst (Fe_3O_4/ Si/**CX4**) were iron (II) sulfate ($FeSO_4{\cdot}7H_2O$, Sigma-Aldrich, 99% purity), sodium hydroxide (NaOH, Synth, 99% purity), tetraethyl orthosilicate (TEOS, Sigma-Aldrich, 98% purity) and (3-glycidyloxypropyl) trimethoxysilane (GLYMO, Sigma-Aldrich, >98% purity). For the synthesis of Biginelli's adducts, the aldehydes were purchased from Sigma-Aldrich and were used as received.

The synthesis of Biginelli adducts was performed in a CEM Discover System (Model No: 908005) microwave reactor operating at 50/60 Hz with a maximum power of 250 W and a microwave frequency of 2455 mHz.

2.2. Synthesis and characterization of materials

Magnetite nanoparticles (Fe_3O_4) were obtained by controlled precipitation of $FeSO_4{\cdot}7H_2O$ (100 mL, 0.1 mol L^{-1}) using NaOH solution (0.45 mol L^{-1}), which was added dropwise until the solution reached pH 12. The brown solid was filtered, washed (50 mL H_2O) and oven dried at 50 °C for 24 h [46].

Modified magnetic nanoparticles were prepared following a published procedure [47]. Typically, 0.5 g Fe_3O_4 nanoparticles were suspended in distilled water (25 mL), methanol (3.75 mL), NaF (1.25 mL of 1% water solution) and GLYMO (135 mL) and stirred for 15 min. After that time, tetraethyl orthosilicate (7.5 mL) was added dropwise to this mixture, which was stirred for 48 h. The obtained material, named Fe_3O_4/Si, was separated by magnetic means, washed with

water and ethanol until a neutral pH was reached and dried in an oven (50 °C for 24 h).

For the synthesis of *p*-sulfonic acid calix[4]arene (**CX4**), 3.5 mmol *p-tert*-butylcalix[4]arene and 15 mL concentrated sulfuric acid were constantly stirred for 4 h at 80 °C. The obtained solid was filtered, washed with ethyl acetate (200 mL) and oven dried at 50 °C for 24 h. The **CX4** was characterized by ^{1}H and ^{13}C nuclear magnetic resonance (NMR) spectroscopy and infrared (FTIR-ATR) spectroscopy (ESI Figs. 1–3), and the data were compared to those reported elsewhere (Supplementary Material) [27,31].

For the incorporation of *p*-sulfonic acid calix[4]arene into the magnetic particles (Fe_3O_4/Si/**CX4**), the methodology proposed by Sayin et al. (2010) was adapted [48]. Thus, 0.15 g **CX4** and 0.112 g K_2CO_3 were stirred in acetonitrile (10 mL) for 30 min. Then, 0.45 g Fe_3O_4/Si was added, and the mixture was refluxed for 73 h. The mixture was acidified with 0.1 mol L^{-1} HCl (2 mL) solution. The solid was magnetically separated with the aid of a magnet and washed with water and ethanol (20 mL each) until a neutral pH was reached. The material was oven dried at 50 °C for 24 h.

The materials were characterized by thermal analysis in a DTG-60 Shimadzu instrument under nitrogen flow (50 mL min^{-1}) in the range of 30–1000 °C at a heating rate of 10 °C min^{-1}. The Fourier transform infrared spectra (FTIR) of the materials (in the form of KBr pellets) were measured using a PerkinElmer FTIR GX spectrometer in the range of 400–4000 cm^{-1} at a resolution of 4 cm^{-1}. SEM and TEM were performed in an FEG – Quanta FEI Electronic Scanning Electron Microscope and in an FEI – 200 kV Tecnai G2-20 – SuperTwin Electronic Transmission Electron Microscope, respectively. X-ray diffraction was performed in a Rigaku Geigerflex model using CuKα radiation (1.5406 Å) with a scanning speed of 2° min^{-1}. The average crystallite sizes were estimated by Scherrer's equation. The specific surface areas (BET) of the samples were analyzed by adsorption of N_2 at 77 K using an Autosorb1-MP Quantachrome instrument. The samples were degassed at 200 °C for 24 h prior to analysis. To identify the phases of iron-containing materials, Mössbauer analyses were performed using a conventional CMTE – MA250 spectrometer with constant acceleration by moving a ^{57}Co source into a Rh matrix.

2.3. Catalytic tests: Synthesis of the Biginelli adducts [dihydropyrimidinones (DHPM's)]

For the catalytic tests, 1.0 mmol of the corresponding aldehyde, 1.5 mmol urea, 1.5 mmol ethyl acetoacetate and 50 mg (0.64 mol%) catalyst (Fe_3O_4/Si/**CX4**) were transferred to a microwave reactor and maintained at atmospheric pressure for 20 min at 90 °C. At the end of the reaction, the product was solubilized in 2 mL of ethanol, and the catalyst was removed with the aid of a magnet. Ethanol was evaporated under reduced pressure, and the material was purified using a filter column and hexane:AcOEt (4:1) mixture as the eluent.

The obtained products were characterized by ^{1}H, ^{13}C NMR and DEPT-135 experiments (Figs. S4–S19) using a Bruker DPX 200 Avance spectrophotometer operating at 200 MHz or 400 MHz for ^{1}H and 50 MHz or 100 MHz for ^{13}C NMR experiments.

2.4. Reuse of the catalyst

At the end of the reaction, the catalyst was removed from the reaction medium with a magnet, washed five times with ethanol and placed to dry at 50 °C in an oven for 24 h. After drying, the material was reused in other catalytic cycles.

3. Results and discussion

3.1. Synthesis and characterization of catalyst

The synthesis of materials with structure and controlled morphology is a challenge for the science of materials. According to the literature [49–51], the synthesis method directly influences the size, shape of the particles obtained and their behavior within a reaction medium. Thus, we can say that the size and morphology of nanoparticles are two important characteristics capable of influencing their electrical, optical and magnetic and mainly catalytic properties. This is because such results allow for a more homogeneous reaction and a faster reaction kinetics due to the morphological uniformity and regularity of the same diameter. In addition, the development of an iron-based core-shell catalyst is interesting, since this can prevent the agglomeration of particles.

In previous studies, we have reported the catalytic effect of *p*-sulfonic acid calix[4]arene (**CX4**), a homogeneous catalyst, for the synthesis of Biginelli adducts [32]. Inspired by these results, we pursued herein to explore the effects of these flexible, bulky acid macrocycles supported by magnetic nanoparticles as heterocatalysts - *p*-sulfonic acid calix[4]arene (**CX4**) on silica-based magnetite particle (Fe_3O_4/Si) surfaces (Fe_3O_4/Si/**CX4**) - in the Biginelli reaction under solvent-free conditions and microwave irradiation (IMO). The magnetic particle-supported *p*-sulfonic acid calix[4]arene (Fe_3O_4/Si/**CX4**) was prepared following the steps shown in Fig. 2.

The first step was the preparation of *p*-sulfonic acid calix[4]arene (**CX4**) according to the published procedure (Fig. 2, step 1) [32,52]. The characterization data for **CX4** are available as Supplementary Material (Figs. S1, S2, and S3).

Magnetite (Fe_3O_4) (Fig. 2, step 2) was prepared *via* controlled precipitation of Fe^{2+} salt with NaOH, which leads to the formation of an oxide with magnetic characteristics in a simple and practical way. The ferrous sulfate is dissociated and partially hydrolyzed to goethite (α-FeOOH) in the presence of atmospheric oxygen. The reaction of goethite and iron(II) hydroxide, in turn, leads to the formation of magnetite [53]. Having the magnetite (Fe_3O_4) in hand, our efforts were to obtain its silicon-covered form (Fe_3O_4/Si) by treating the former with tetraethyl orthosilicate (TEOS) and GLYMO in the presence of 1% NaF (Fig. 2, step 3).

CX4 was attached to Fe_3O_4/Si by the opening of the epoxide ring (Fig. 2, step 4) according to the methodology proposed by Sayin et al. (2010, 2017) [48,54]. This procedure prevents the leaching of **CX4,** allowing reuse for several catalytic cycles.

Thermogravimetric analysis indicated a mass loss of 4% for Fe_3O_4. For the Fe_3O_4/Si sample, the mass loss was 23%. Mass losses between 50 and 250 °C can be attributed to adsorbed water molecules. Mass-loss events that start at temperatures above 250 °C and remain constant up to 750 °C correspond to water loss due to the condensation process of silanols on the surface (Fig. 3).

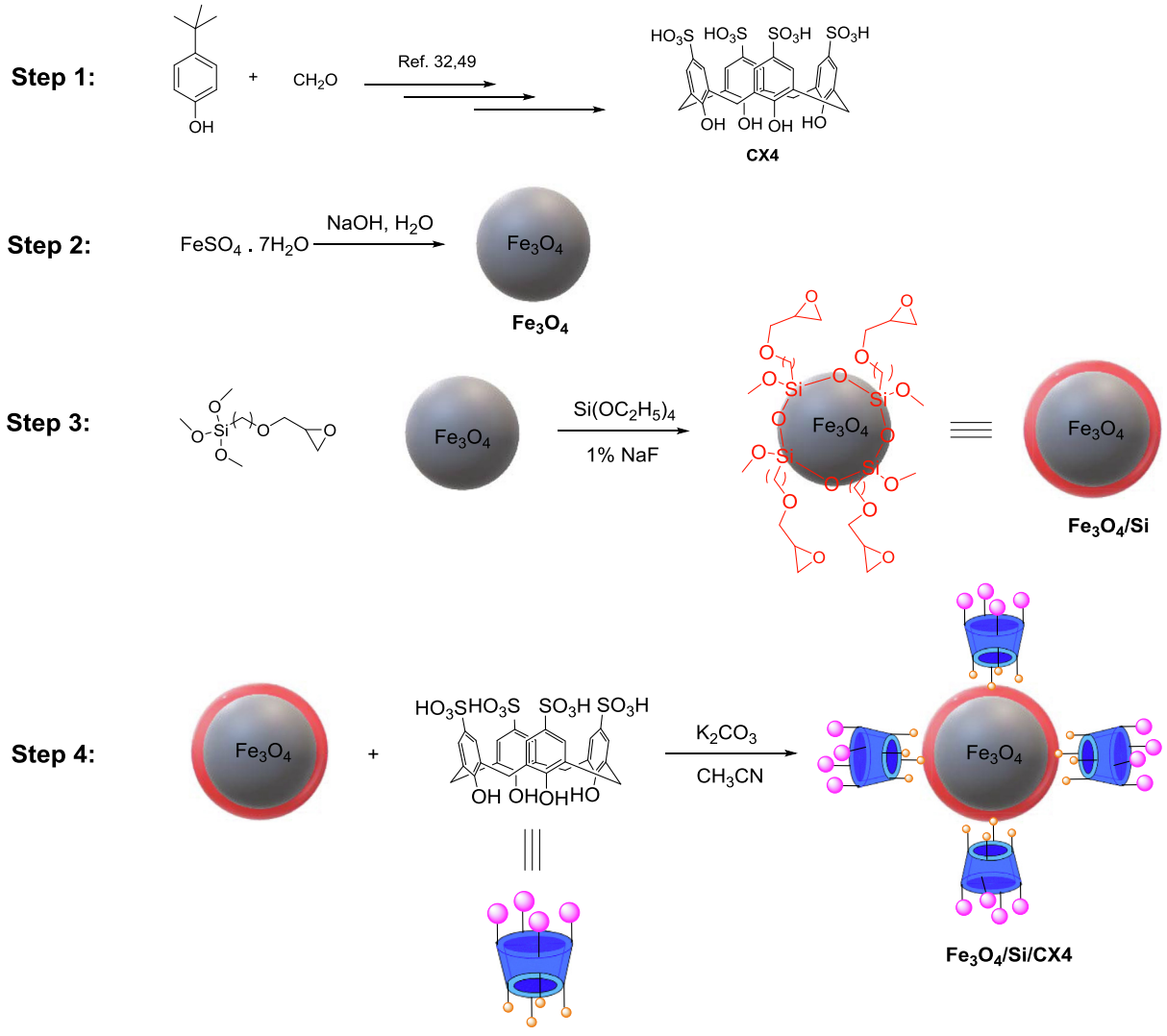

Fig. 2 Steps involved in the preparation of magnetic nanoparticles supported *p*-sulfonic acid calix[4]arene (Fe_3O_4/Si/**CX4**).

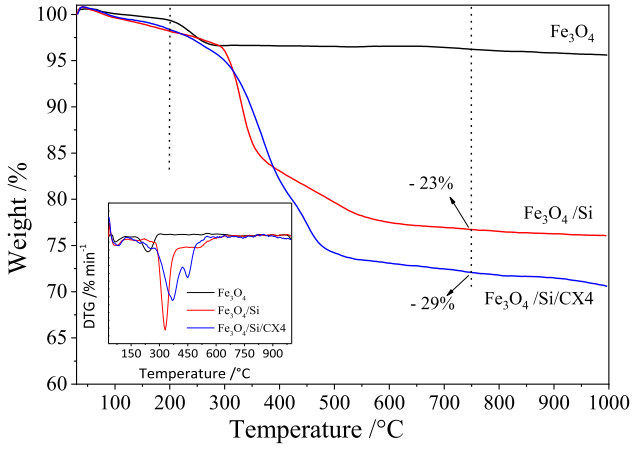

Fig. 3 TGA curves of Fe_3O_4, Fe_3O_4/Si and Fe_3O_4/Si/**CX4.** (Detail: Curve DTG).

TGA of Fe_3O_4/Si/**CX4** shows two stages of decomposition: the first stage below 200 °C (2% loss of weight), corresponding to water loss, and the second stage between 200 and 700 °C (25% loss), which is attributed to the condensation process of the silanol groups and the decomposition of the organic groups of the **CX4** anchored on the surface of the silica. The mass loss for this sample was approximately 30%. Approximately 5.4% of this loss corresponds to **CX4**, which is bound in the magnetic particle.

To determine the concentrations of acid groups in the samples, titrations were performed. In this experiment, 10 mg solid was added to 10 mL 0.01 M KOH solution as an exchange agent. After equilibration (4 h), the solution was filtered and titrated with 0.01 M HCl. The acid capacities of the materials were 0.23 and 0.35 mmol H^+ g^{-1} for Fe_3O_4 and Fe_3O_4/Si, respectively. The acidity can be related to the hydroxyl groups [55]. The addition of *p*-sulfonic acid calix[4]arene groups nearly doubled the acid capacity of the Fe_3O_4/Si/**CX4** catalyst. The concentration of acid groups was 0.70 mmol H^+ g^{-1}. This result indicates that the C-SO_3 group bound to the surface of the material can generate acidity. This property is important

for catalytic processes involving Biginelli adducts. Similar results for the proton acidity of materials involving magnetic nanoparticles and sulfonic groups were found in the literature [44,56,57].

The FT-IR spectrum of Fe_3O_4/Si/**CX4** is shown in Fig. 4. The bands at 459 and 558 cm^{-1} belong to the stretching vibration mode of Fe–O bonds in Fe_3O_4. Bands corresponding to asymmetric, symmetric, and bending vibrations for the Si–O–Si moiety are observed at 1000–1300 (broad), 798, and 459 cm^{-1}, respectively. Si–OH groups are detected by the broad band at 2800–3700 cm^{-1}. The spectrum possesses peaks of the stretching vibration of amines at 1641 cm^{-1}. The band at 1446 cm^{-1} is attributed to the bending vibration of aromatic C═C bonds of calix[4]arene. The vibrational bands at 2942 and 2877 cm^{-1} are attributed to the asymmetric and symmetric stretching vibrations of $–CH_2–$ groups present in the covalently modified calixarene, respectively. Peaks due to the symmetric and asymmetric vibrations of S–O that derive from the calix[*n*]arene sulfonic acids appear at 944 cm^{-1}. The frequency values correspond to the symmetric and anti-symmetric stretching vibrations of S═O bonds in the C–SO_3 group at 1080 cm^{-1} [40,42,47,58,59].

The powder XRD pattern of the synthesized material is shown in Fig. 5. The diffractogram of the synthesized material showed peaks related to crystalline phases (according to the Joint Committee on Powder Diffraction Standards (JCPDS)) of Fe_3O_4 (JCPD-19-629), FeOOH (JCPD-29-713), γ-Fe_2O_3 (JCPD-39-1346) and FeSi (JCPD-2-1267). Comparing the diffractograms, it is possible to verify that silanization and functionalization did not alter the structural characteristics of the iron oxide nanocomposites. However, a slight loss of crystallinity and an extra peak at approximately 22°, characteristic of amorphous silica, were observed, as expected. As a function of the iron oxide measuring process, an increase in the mean crystallite size and a reduction in the BET area were observed (17 nm, 20 m^2g^{-1} for Fe_3O_4 and 22 nm, 14 m^2g^{-1} for Fe_3O_4/Si/**CX4**).

Considering that Fe_3O_4 and γ-Fe_2O_3 have the same diffraction pattern, the identification of these species was only possible by Mössbauer spectroscopy experiments (Fig. 6A).

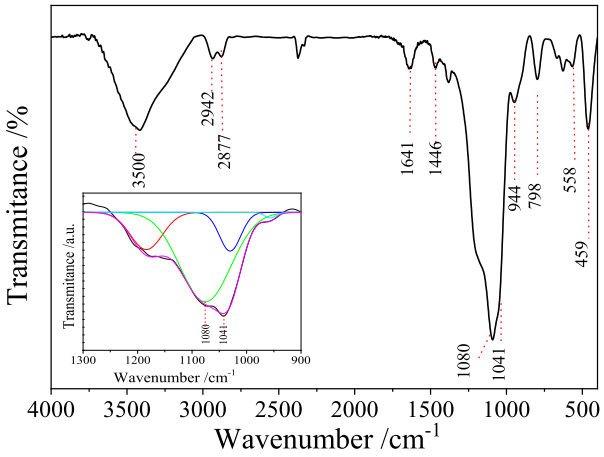

Fig. 4 FTIR-ATR spectrum of Fe_3O_4/Si/**CX4**. Detail: Deconvolution of the bands in the region between 1300 and 850 cm^{-1}.

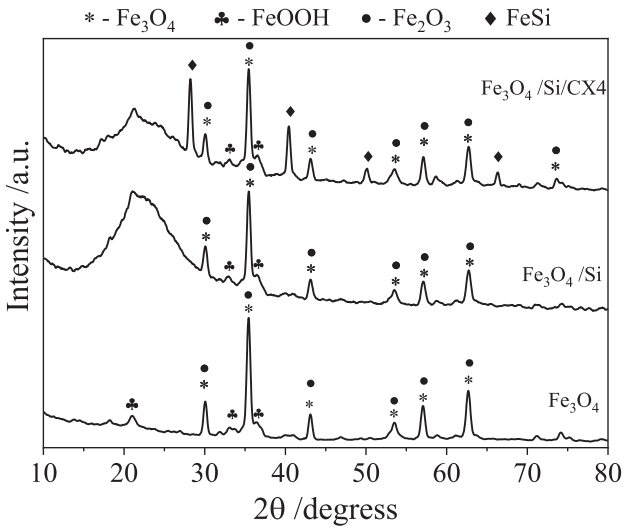

Fig. 5 Powder XRD pattern of the Fe_3O_4, Fe_3O_4/Si, and Fe_3O_4/Si/**CX4.**

Moreover, those results showed that the prepared magnetite (Fe_3O_4) is instead a mixture of iron oxides. The results indicate that approximately 30% of the sample is oxidized to γ-Fe_2O_3 and 28% to α-FeOOH and a highly dispersed Fe^{3+} superparamagnetic species (9%) (Fig. 6B). The more reactive phases of Fe_3O_4 are oxidized by air at room temperature to produce γ-Fe_2O_3 [60].

The hyperfine parameters are presented in Table S1 (ESI). The Mössbauer spectrum of Fe_3O_4 shows a sextet related to the γ-Fe_2O_3 phase. The magnetite coated with silica (Fe_3O_4/Si) showed, that the relative area of the γ-Fe_2O_3 sextet increases (from 31 to 42%). The same was true for Fe_3O_4/Si/**CX4** (47%).

The Fe_3O_4 has sextets assigned to the octahedral and tetrahedral sites of the magnetite phase, Fe_3O_4, with 19 and 13% of the area, respectively. For Fe_3O_4/Si, the areas relative to the octahedral and tetrahedral phases were 15 and 7%, respectively. The modification of the structure with *p*-sulfonic acid calix[4]arene groups practically does not alter the areas related to the octahedral and tetrahedral phases of the magnetite. This was expected since the magnetic material is completely coated with silica and p-sulfonic acid calix[4]arene, thereby reducing the exposure to oxygen in the air.

SEM images of Fe_3O_4 (Fig. 7) show the formation of irregular nanoparticles with different morphological characteristics, some with rounded aspects and some in the form of needles, which may be justified by the presence of α-FeOOH and γ-Fe_2O_3 in the material. The mean particle size is 80 nm. For the Fe_3O_4/Si/**CX4** sample, it is observed that the particles are agglomerated. TEM (Fig. 8) images also show the formation of agglomerates composed of the overlapping and joining of several smaller particles. In general, particles smaller than 100 nm can be observed but are agglomerated. The changes in the shape and size of the Fe_3O_4/Si/**CX4** are expected because of the covalent modification, and our results agree well with the literature [40].

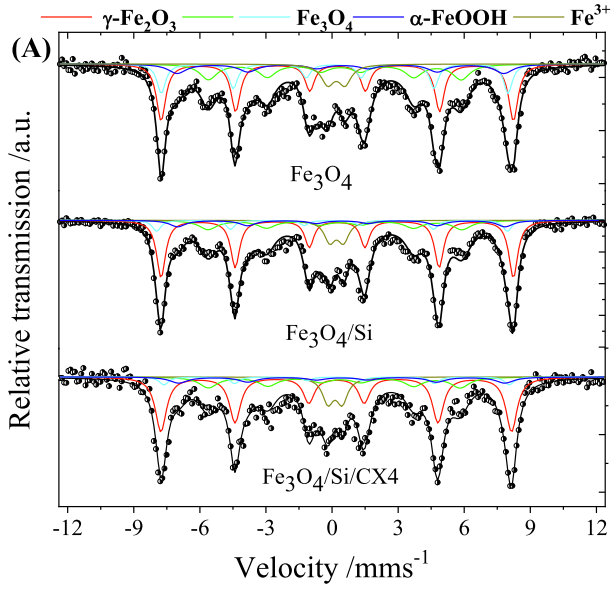

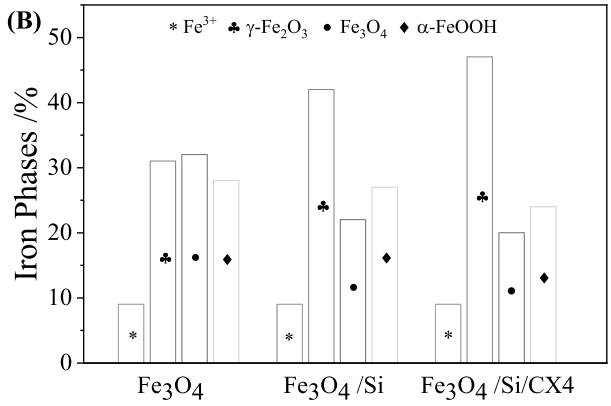

Fig. 6 **(A)** Mössbauer spectra of Fe_3O_4, Fe_3O_4/Si, and Fe_3O_4/Si/**CX4**; (B) Iron phases distribution.

3.2. Catalytic activity

In the work developed by da Silva et al. (2011) [32], it was observed that **CX4** exerted a catalytic role in the reaction involving Biginelli adducts; however, recovery of the catalyst was difficult. In this work, we chose to support the homogeneous catalyst in a magnetic matrix, the magnetite (Fe_3O_4), which facilitates the recovery of the catalyst to be used again in other reaction cycles. The reaction was carried out in the presence and absence of solvent using heating by means of microwave irradiation. The following reagents were used for the optimization of this reaction: benzaldehyde, ethyl acetoacetate and urea. The reaction occurred in the presence of 0.64 mol% catalyst for 20 min at 90 °C. A general outline is presented below.

The results indicate that a higher yield of 88% is obtained when working in the absence of solvent (Table 1). This result was verified when **CX4** was used in a homogeneous medium by Silva et al. (2011) [32].

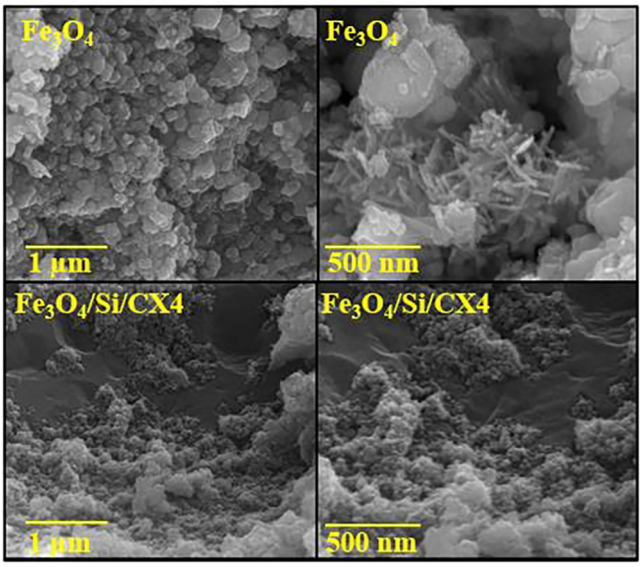

Fig. 7 SEM images of Fe_3O_4 magnetic nanoparticles (up) and Fe_3O_4/Si/**CX4** (below).

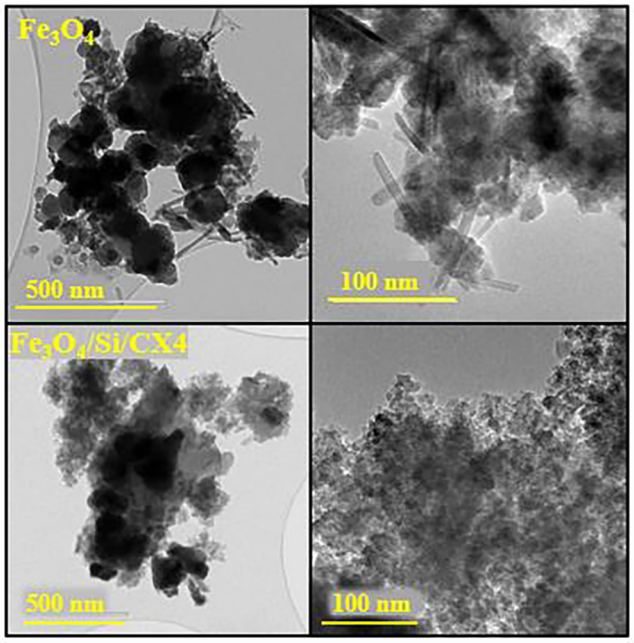

Fig. 8 TEM images of Fe_3O_4 magnetic nanoparticles (up) and Fe_3O_4/Si/**CX4** (below).

The influence of the catalyst content was also evaluated (Table 2). The results indicate that 0.64 mol% catalyst leads to greater conversion of the reactants. Assays in the absence of a catalyst and in the presence of Fe_3O_4 alone were also performed, and the data indicate that the presence of **CX4** in the support (Fe_3O_4/Si/**CX4**) is important for the reaction since acid sites are required for the reaction to occur. Assays using only **CX4** (homogeneous catalysis) were also performed. The results indicate that a higher yield is obtained when using Fe_3O_4/Si/**CX4** as the catalyst. The Lewis acid nature of Fe_3O_4 has already been reported in the literature, and together

Table 1 Influence of solvent in Biginelli reaction.

Solvent	Yield (%)
Acetonitrile	18%
Ethanol	64%
Ethyl lactate	ND
Diethyl carbonate	ND
Without solvent	88

Table 2 Influence of homogeneous (**CX4**) and heterogeneous [Fe_3O_4/Si/**CX4**] catalysts in Biginelli Reaction.

Catalyst		Yield (%)
Free		28
Fe_3O_4		43
Fe_3O_4/Si		45
CX4-Homogeneous		60
Fe_3O_4/Si/**CX4**	0,30 mol%	60
	0,64 mol%	88
	1,00 mol %	67

with the Brønsted acidity of **CX4**, it contributes significantly to the increase in reaction yield. This may be related to a synergistic effect occurring between the Lewis and Brønsted acid sites of Fe_3O_4/Si/**CX4**. That is, the presence of both types of acid sites is important for an increase in yield for this reaction.

The effect of the type of heating was also evaluated (Table 3). It was possible to verify that when using microwave irradiation and an open tube, the highest yield (88%) was obtained. With regard to conventional heating, achieving a 69% yield required 30 h of reaction. For microwave heating, 88% yield was obtained in 20 min with an open bottle and 56% with the bottle closed. One hypothesis capable of explaining these results is that during the reaction, water molecules are formed. With the flask open, these molecules can escape from the reaction medium; thus, the equilibrium shifts toward the formation of Biginelli adducts. In contrast, for the sealed tube, the water molecules remain in the reaction medium, thus allowing a less effective equilibrium displacement in the direction of product formation.

Leaching tests were also performed. Fe_3O_4/Si/**CX4** was maintained in contact for 5 min with ethyl acetoacetate under microwave irradiation, and after this period, the catalyst was withdrawn from the reaction system, and the other reagents were added to the reactor. The reaction was continued for another 20 min under microwave irradiation. The yield of the reaction was less than 20%. These data indicate that there was no loss of acid groups to the reaction medium. Therefore, we can say that the methodology to fix **CX4** to magnetic nanoparticles was efficient and that the reaction evaluated is heterogeneous.

Table 3 Influence of type of heating in yield of the Biginelli reaction.

Type of heating		Yield (%)
30 h Conventional		69
Microwave	20 min open tube	88
	25 min sealed tube	56

After verifying the high catalytic activity, we tested the Fe_3O_4/Si/**CX4** reuse capacity. The catalyst remained stable for 5 cycles. In the last cycle, the reaction yield was 84%, only 4% less that of the first cycle (Fig. 9). In this way, it can be concluded that in these reaction conditions, the catalyst stability is satisfactory. The reused material was stored for 3 months, and after this period, it was used again in the reaction. The obtained yield was 78%. This result may indicate that even after aging, the catalyst does not lose its activity. The material characterized by IR before use (fresh) and after reuse and storage for 3 months (aged) showed the same characteristic bands (FTIR Fig. S20).

The effect of the aldehyde on the reaction was also evaluated (Table 4). Reactions were conducted using microwave irradiation at 90 °C (open tube), 0.64% catalyst in the absence of a solvent. It is noteworthy that the choice of these aldehydes was made selecting those with electron-withdrawing and electron-donating substituents and heteroaromatic and aliphatic aldehydes. It has been found that the catalyst can be used for any type of aldehyde, with the electron-donating, electron-withdrawing or heteroaromatic substituents. It can further be noted that yields using aldehydes with electron-withdrawing groups (55–87%) were lower compared to those with electron-donating substituents (73–88%).

Our results were similar or higher than those reported by Zamani and Izadi [61] and Zamani et al. [62]. These authors obtained 75–90% and 80–97% Biginelli adducts using sulfonated phenylacetic acid and 3-mercaptopropanoic acid (MPA) anchored to Fe_3O_4 nanoparticles, respectively. However, it is noteworthy to mention that in both Zamani articles the nanoparticles employed bear 7-fold more acidic sites than Fe_3O_4/Si/**CX4** obtained in this work. Biginelli's adducts were characterized by ^1H, ^{13}C NMR and DEPT-135 (Figs. S4–S19). Table 5 presents studies using different catalysts for a reaction involving Biginelli adducts.

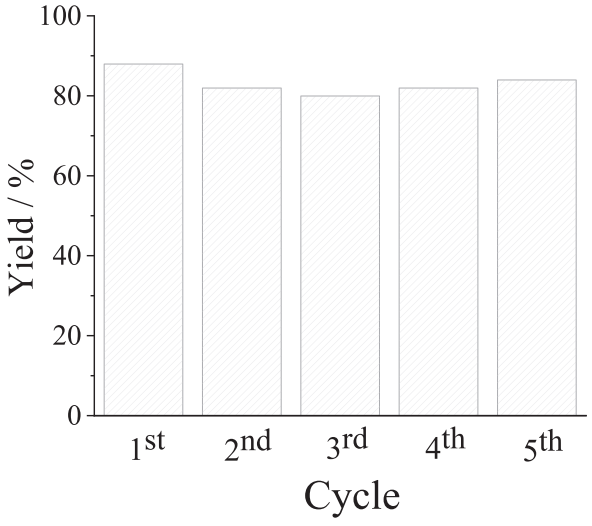

Fig. 9 The yields of Biginelli adduct **BA1** using Fe_3O_4/Si/**CX4** in five cycles. (Yield for the isolated product).

Table 4 Fe_3O_4/Si/**CX4** catalyzed the one-pot synthesis of Biginelli adducts.

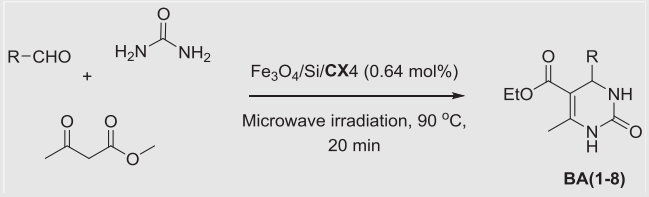

Entry	R	Product	Yield (%)
1		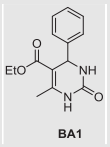 BA1	88
2	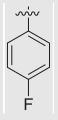	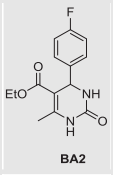 BA2	87
3	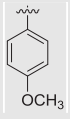	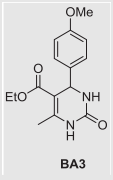 BA3	88
4	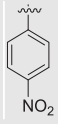	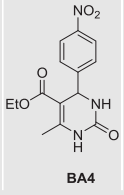 BA4	55
5		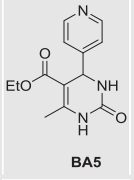 BA5	73
6		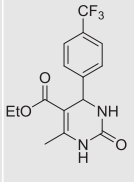 BA6	62
7		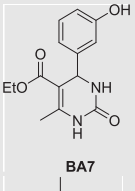 BA7	80
8		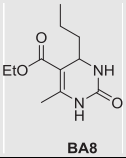 BA8	87

Table 5 Comparison of maximum yield using Fe_3O_4/Si/**CX4** and those obtained by other catalysts described in the literature.

Catalyst	Temp °C	TimeMin	[Acid sites] mmol H^+ g^{-1}	Cycles	Yield	Ref
Fe_3O_4/Si/**CX4**	90	20	0.70	5	88	–
Fe_3O_4/PAA-SO_3H	25	120	3.71	6	90	[61]
Fe_3O_4/SMPA	25	120	3.92	6	95	[62]
Montmorillonite clay	78	120	0.56	4	98	[63]
Acidic ionic liquid immobilized on Fe_3O_4	100	30	0.44	8	95	[64]
ZnO@SBA-15	65	150	–	5	96	[65]
Ionic liquid immobilized on MCM-41@Cu	80	120	–	6	90	[66]
MCM-41-R-SO_3H	85	360	1.10	5	92	[67]

4. Conclusions

In conclusion, a magnetic material synthesized by the precipitation method was synthesized and modified with calixarene. This material was used as a heterogeneous catalyst in the reaction to obtain Biginelli adducts, which were obtained in satisfactory yields. The catalyst can be removed from the reaction medium by simply and rapidly employing a magnet, and it was recovered and reused for five cycles without loss of catalytic activity.

Declaration of Competing Interest

None.

Acknowledgments

This work was made possible because of the financial support by the Brazilian agencies Conselho Nacional de Desenvolvimento Científico e Tecnológico (CNPq), Coordenação de Aperfeiçoamento de Pessoal de Nível Superior (CAPES, Financial code 001) and Fundação de Amparo à Pesquisa do Estado de Minas Gerais (FAPEMIG). AdF and MHA are supported by Research Fellowships from CNPq. The authors are thankful to Anislay Alvarez Hernandez and Maite Docampo (University of North Texas, USA) for critical reading of the manuscript and to Pró-reitoria de Pesquisa of Universidade Federal de Minas Gerais (UFMG) for the financial assistance.

Appendix A. Supplementary data

Supplementary data to this article can be found online at https://doi.org/10.1016/j.jscs.2019.05.005.

References

[1] R.A. Sheldon, Chem. Soc. Rev. 41 (2012) 1437–1451.
[2] K. Wilson, J.H. Clark, Pure Appl. Chem. 72 (2000) 1313–1319.
[3] K. Tanabe, W.F. Ho, Appl. Catal. A Gen. 181 (1999) 399–434.
[4] E. Guibal, Prog. Polym. Sci. 30 (2005) 71–109.
[5] L. Yin, J. Liebscher, Chem. Rev. 107 (2007) 133–173.
[6] M. Zabeti, W.M.A. Wan Daud, M.K. Aroua, Fuel Process. Technol. 90 (2009) 770–777.
[7] D. Wang, D. Astruc, Chem. Rev. 114 (2014) 6949–6985.
[8] C.J. Welch, J. Albaneze-Walker, W.R. Leonard, M. Biba, J. DaSilva, D. Henderson, B. Laing, D.J. Mathre, S. Spencer, X. Bu, T. Wang, Org. Process Res. Dev. 9 (2005) 198–205.
[9] H.J. Federsel, Drug Discov. Today. 11 (2006) 966–974.
[10] A.H. Lu, E.L. Salabas, F. Schüth, Angew. Chem. Int. Ed. 46 (2007) 1222–1244.
[11] D.W. Li Lai, Qiang Xie, Lina Chi, Gu. Wei, J. Colloid Interface Sci. 465 (2016) 76–82.
[12] H. Aono, H. Hirazawa, T. Naohara, T. Maehara, H. Kikkawa, Y. Watanabe, Mater. Res. Bull. 40 (2005) 1126–1135.
[13] R. Fan, X.H. Chen, Z. Gui, L. Liu, Z.Y. Chen, Mater. Res. Bull. 36 (2001) 497–502.
[14] C. Balasubramaniam, Y.B. Khollam, I. Banerjee, P.P. Bakare, S.K. Date, A.K. Das, S.V. Bhoraskar, Mater. Lett. 58 (2004) 3958–3962.
[15] S.A. Corr, Y.K. Gun'ko, A.P. Douvalis, M. Venkatesan, R.D. Gunning, J. Mater. Chem. (2004) 944–946.
[16] J. Xu, H. Yang, W. Fu, K. Du, Y. Sui, J. Chen, Y. Zeng, M. Li, G. Zou, J. Magn. Magn. Mater. 309 (2007) 307–311.
[17] C.R. Lin, Y.M. Chu, S.C. Wang, Mater. Lett. 60 (2006) 447–450.
[18] D. Thapa, V.R. Palkar, M.B. Kurup, S.K. Malik, Mater. Lett. 58 (2004) 2692–2694.
[19] V. Polshettiwar, R. Luque, A. Fihri, H. Zhu, M. Bouhrara, J.M. Basset, Chem. Rev. 111 (2011) 3036–3075.
[20] M.B. Gawande, P.S. Branco, R.S. Varma, Chem. Soc. Rev. 42 (2013) 3371–3393.
[21] D.M. Homden, C. Redshaw, Chem. Rev. 108 (2008) 5086–5130.
[22] J.B. Simões, D.L. Silva, A. De Fátima, S.A. Fernandes, Curr. Org. Chem. 16 (2012) 949–971.
[23] M. Raynal, P. Ballester, A. Vidal-Ferran, P.W.N.M. Van Leeuwen, Chem. Soc. Rev. 43 (2014) 1660–1733.
[24] M. Raynal, P. Ballester, A. Vidal-Ferran, P.W.N.M. Van Leeuwen, Chem. Soc. Rev. 43 (2014) 1734–1787.
[25] C. Deraedt, D. Astruc, Coord. Chem. Rev. 324 (2016) 106–122.
[26] M. Durmaz, E. Halay, S. Bozkurt, J. Org. Chem. 14 (2018) 1389–1412.
[27] J.B. Simões, Â. De Fátima, A.A. Sabino, F.J.T. De Aquino, D. L. Da Silva, L.C.A. Barbosa, S.A. Fernandes, Org. Biomol. Chem. 11 (2013) 5069–5073.
[28] P.A.D.S. Abranches, W.F. De Paiva, Â. De Fátima, F.T. Martins, S.A. Fernandes, J. Org. Chem. 83 (2018) 1761–1771.
[29] J.B. Simões, Â. De Fátima, A.A. Sabino, L.C. Almeida Barbosa, S.A. Fernandes, RSC Adv. 4 (2014) 18612–18615.
[30] N.A. Liberto, J.B. Simï¿øes, S. de Paiva Silva, C.J. da Silva, L.V. Modolo, Angelo de Fátima, L.M. Silva, M. Derita, S. Zacchino, O.M.P. Zuïga, G.P. Romanelli, S.A. Fernandes, Bioorg. Med. Chem. 25 (2017) 1153–1162.
[31] D.L. Da Silva, B. Silva Terra, M. Ribeiro Lage, A. Lúcia Tasca Góis Ruiz, C. Capeletti Da Silva, J. Ernesto De Carvalho, J. Walkimar De Mesquita Carneiro, F. Terra Martins, S. Antonio Fernades, Â. De Fátima, Org. Biomol. Chem. 13 (2015) 3280–3287.
[32] D.L. Da Silva, S.A. Fernandes, A.A. Sabino, Â. De Fátima, Tetrahedron Lett. 52 (2011) 6328–6330.

[33] D.L. Da Silva, F.S. Reis, D.R. Muniz, A.L.T.G. Ruiz, J.E. De Carvalho, A.A. Sabino, L.V. Modolo, Â. De Fátima, Bioorg. Med. Chem. 20 (2012) 2645–2650.
[34] Â. de Fátima, T.C. Braga, L. da S. Neto, B.S. Terra, B.G.F. Oliveira, D.L. da Silva, L.V. Modolo, J. Adv. Res. 6 (2015) 363–373.
[35] L.P. Horta, Y.C.C. Mota, G.M. Barbosa, T.C. Braga, I.E. Marriel, Â. De Fátima, L.V. Modolo, J. Braz. Chem. Soc. 27 (2016) 1512–1519.
[36] P. Sarkar, C. Mukhopadhyay, Green Chem. 18 (2016) 6556–6563.
[37] A. Acharya, K. Samanta, C.P. Rao, Coord. Chem. Rev. 256 (2012) 2096–2125.
[38] S. Tanwar, M.C. Chuang, K.S. Prasad, J.A.A. Ho, Green Chem. 14 (2012) 799–808.
[39] D. Xiong, M. Chen, H. Li, Chem. Commun. (2008) 880–882.
[40] N. Narkhede, B. Uttam, R. Kandi, C.P. Rao, ACS Omega 2018 (3) (2018) 229–239.
[41] S. Sayin, E. Yilmaz, M. Yilmaz, Org. Biomol. Chem. 9 (2011) 4021–4024.
[42] S. Sayin, M. Yilmaz, J. Chem. Eng. Data. 56 (2011) 2020–2029.
[43] E. Akceylan, A. Uyanik, S. Eymur, O. Sahin, M. Yilmaz, Appl. Catal. A Gen. 499 (2015) 205–212.
[44] S. Sayin, M. Yilmaz, Tetrahedron 70 (2014) 6669–6676.
[45] L.H.S. Matos, F.T. Masson, L.A. Simeoni, Eur. J. Med. Chem. 143 (2018) 1779–1789.
[46] D.D. Suppiah, S.B. Abd Hamid, J. Magn. Magn. Mater. 414 (2016) 204–208.
[47] S. Sayin, F. Ozcan, M. Yilmaz, J. Hazard. Mater. 178 (2010) 312–319.
[48] S. Sayin, F. Ozcan, M. Yilmaz, A. Tor, S. Memon, Y. Cengeloglu, Clean Soil Air Water 38 (2010) 639–648.
[49] L. León Félix, J.A.H. Coaquira, M.A.R. Martínez, G.F. Goya, J. Mantilla, M.H. Sousa, L.D.L.S. Valladares, C.H.W. Barnes, P.C. Morais, Sci. Rep. 7 (2017) 1–8.
[50] J. Tu, J. Yuan, S. Kang, Y. Xu, T. Wang, New J. Chem. 42 (2018) 10861–10867.
[51] Á. de J. Ruíz-Baltazar, S.Y. Reyes-López, M. de L. Mondragón-Sánchez, A.I. Robles-Cortés, R. Pérez, Results Phys. 12 (2019) 989–995.
[52] C.D. Gutsche, Calixarenes: An Introduction, 2nd ed., UK, 2008.
[53] A.P.C. Teixeira, J.C. Tristão, M.H. Araujo, L.C.A. Oliveira, F. C.C. Moura, J.D. Ardisson, C.C. Amorim, R.M. Lago, J. Braz. Chem. Soc. 23 (2012) 1579–1593.
[54] S. Sayin, M. Yilmaz, RSC Adv. 7 (2017) 10748–10756.
[55] V.O. Leone, M.C. Pereira, S.F. Aquino, L.C.A. Oliveira, S. Correa, T.C. Ramalho, L.V.A. Gurgel, A.C. Silva, New J. Chem. 42 (2018) 437–449.
[56] M.L. Testa, V. La Parola, A.M. Venezia, Catal. Today. 223 (2014) 115–121.
[57] J. Kothandapani, A. Ganesan, S. Selva Ganesan, Tetrahedron Lett. 56 (2015) 5568–5572.
[58] M. Sheykhan, A. Yahyazadeh, L. Ramezani, Mol. Catal. 435 (2017) 166–173.
[59] L. Shmygleva, N. Slesarenko, A. Chernyak, E. Sanginov, A. Karelin, A. Pisareva, R. Pisarev, Y. Dobrovolsky, Int. J. Electrochem. Sci. 12 (2017) 4056–4076.
[60] I.T. Cunha, I.F. Teixeira, J.P. Mesquita, J.D. Ardisson, I. Binatti, F.V. Pereira, R.M. Lago, J. Braz. Chem. Soc. 27 (2016) 363–371.
[61] F. Zamani, E. Izadi, Catal. Commun. 42 (2013) 104–108.
[62] F. Zamani, S.M. Hosseini, S. Kianpour, Solid State Sci. 26 (2013) 139–143.
[63] A. Phukan, S.J. Borah, P. Bordoloi, K. Sharma, B.J. Borah, P.P. Sarmah, D.K. Dutta, Adv. Powder Technol. 28 (2017) 1585–1592.
[64] J. Safari, Z. Zarnegar, New J. Chem. 38 (2014) 358–365.
[65] M.A. Douzandegi Fard, H. Ghafuri, A. Rashidizadeh, Microporous Mesoporous Mater. 274 (2019) 83–93.
[66] N. Yao, M. Lu, X.B. Liu, J. Tan, Y.L. Hu, J. Mol. Liq. 262 (2018) 328–335.
[67] G.H. Mahdavinia, H. Sepehrian, Chinese Chem. Lett. 19 (2008) 1435–1439.